6th International Conference on Advances in Experimental Structural Engineering
11th International Workshop on Advanced Smart Materials and Smart Structures Technology
August 1-2, 2015, University of Illinois, Urbana-Champaign, United States

Numerical Study on the Benefits of Base Isolation for Blast Loading

R. Zhang[1], B.M. Phillips[2]

1 Ph.D. Student, Dept. of Civil and Environmental Engineering, University of Maryland, College Park, United States. E-mail: rzhang15@umd.edu
2 Assistant Professor, Dept. of Civil and Environmental Engineering, University of Maryland, College Park, United States. E-mail: bphilli@umd.edu

ABSTRACT
Over the past few decades, researchers have developed many supplemental structural control technologies to improve the responses of structures subjected to seismic excitations. Although blast and seismic loading are two different phenomena from a fundamental physics perspective, seismic control strategies that safely concentrate deflection or safely dissipate energy on the global structure hold some merit for blast loading. Base isolation, one of the most robust and popular passive control technologies, has significant potential to mitigate damage from other impulsive sources such as blast. The goals of this study can be summarized as: (1) demonstrate the potential for base isolation to protect from blast loads and (2) improve the response of base-isolated structures under blasts without compromising seismic protection. Due to the unpredictability of blast loads, independent of seismic risk, robust performance is required under a wide range of charge weights. Through numerical simulations of a low-rise structure, the beneficial effects of using base isolation to reduce interstory drifts and absolute story accelerations seen in earthquake engineering were also observed for blast loading. Furthermore, supplemental control devices were able to maintain nominal base isolation performance under smaller excitations while restricting damaging base displacements under larger excitations.

KEYWORDS: *blast loading, base isolation, structural control, nonlinear bumpers.*

1. INTRODUCTION

Many of the damaging effects of a blast come from the shock wave created when the atmosphere is pushed back by a compressive pulse travelling outward from the center of the explosion [1]. The front of the wave, also known as the shock front, has an overpressure much higher than the ambient pressure. The shock front causes the local pressure to increase to the peak incident pressure followed by a sharp decay in local pressure as the front propagates outward [2]. Shock waves will reflect off surfaces in their path, including the ground, nearby structures, or interior surfaces of a structure, creating reflected shock waves at higher pressure (i.e., reflected overpressure) and velocity. Buildings experience the effects of blasts in several stages. The initial blast wave typically shatters windows and causes other damage to the building façade. In the second stage, the blast wave enters the building and exerts pressure on the structure. When directed upward, this pressure may be extremely damaging to slabs and columns because it acts counter to the design used to resist gravity loads. Finally, the building frame is loaded globally and responds as it would to a short-duration, high-intensity earthquake [3].

The two major parameters which govern the type and degree of damage are the charge weight and distance from the blast to the target. These parameters will also influence what blast-resistant features must be provided to mitigate damage and loss of life. For example, smaller explosives with short standoff distances, e.g., due to a breach in security measures, can destroy load-bearing members leading to a progressive collapse. Larger explosives at longer standoff distances, e.g., due to vehicle delivery methods outside of the structure, will produce more uniform loading over the surface of the building, causing both local and global excitation. Many researchers have proposed local protection strategies against blast loading including sacrificial claddings [4] and foams [5] that can limit both debris and severe structural member damage. With adequate local protection, global behavior becomes significant. This paper will focus on medium to long standoff distances where the global energy absorption and dissipation can play a beneficial role in the protection of the structure from blasts.

Though the loading due to medium to long standoff distance blasts may be somewhat uniform, as typical of seismic loading, seismic design should not be mistaken as redundant to blast design [3]. Blast loads are not proportional to the mass of the structure and therefore may not be distributed to the diaphragms or structural

frame uniformly. The design detailing for seismic loading, including zones of plastic hinge formation, may not be effective under this highly unpredictable loading. However, base-isolation designed for seismic loading bears promise for blast loading. Base-isolation alters the dominate global mode shape of the structure to concentrate deformation at the base level and produce more uniform behavior of the superstructure, even under non-uniform loading. Such change in the global dynamic behavior of the structure can potentially reduce interstory drifts and absolute accelerations, a potential boon for the global protection of buildings under blast loading. Furthermore, base-isolation is not overly sensitive to changes in structural dynamics in contrast to many other structural control technologies, providing robustness even in the face of local damage (e.g., stiffness loss). A challenge for these systems is that large base displacements experienced under severe earthquakes (or blasts) could be damaging to the isolation bearings.

This study investigates the potential for base isolation under blast loads. Further improvements are sought to reduce the base displacements, namely supplemental passive devices are installed on the base level. The devices are chosen to be robust, maintaining function under a damaging blast. Furthermore, due to the unpredictability of blast loads, independent of seismic risk, robust performance under a wide range of scaled standoff distances is required. The goal of this study is to (1) demonstrate the potential for base isolation to protect from blast loads and (2) improve the responses of base-isolated structures under blasts without compromising the innate seismic protection.

2. BASE ISOLATION AND PASSIVE IMPROVEMENTS

Passive base isolation is one of the most successful and widely accepted structure control technologies used to enhance the performance of structures subjected to ground motions [6]. Base isolation shifts the fundamental period of the structure out of the range of the dominant excitation energy and also increases the energy-absorbing capacity of the structure at the base [7, 8]. However, large base displacements induced by the low horizontal stiffness of base isolators can potentially exceed the allowable limits of structural designs causing challenges such as impact with moat walls or damage to the base isolators [9, 10]. Excessive base displacements would be particularly challenging for blast loading, where it is difficult to accurately predict the magnitude and standoff distance of the blast and thus difficult to select a base-level stiffness that balances base isolation performance and base displacement limits. Therefore, the effective control of the base displacements must be addressed to improve base isolation function under unpredictable loading scenarios. Passive devices are the most robust and thus most attractive alternative under intense blast loading or severe earthquakes. In this research, nonlinear bumpers installed between the base and moat wall are proposed.

This study investigates the performance of base isolation through a 5-story base-isolated building model equipped with nonlinear bumpers on the base level subjected to both ground excitations and blasts. The equations of motion for the second-order dynamic system are separated into linear and nonlinear terms. The linear terms are expressed as a linear state-space model. The nonlinear terms (from the nonlinear bumper) are added as a feedback control loop to the linear state-space model. Numerical integration for seismic excitation is performed using a 4^{th} order Runge-Kutta scheme with a fixed time step of 1/10000 seconds. Numerical integration for blast loading is performed using a 4^{th}-5^{th} order Dormand-Prince with a variable time step. All simulations are performed using MATLAB's SIMULINK environment.

2.1 Base-isolated Structure Model

The 5-story base-isolated structure used in the study is adapted from [7, 11] as a basic representation of simple low-rise structures. The superstructure parameters from these studies are reported for a one-third scale model and have been scaled up to represent a full-scale superstructure herein. The fundamental natural period of the superstructure (fixed-base structure) is 0.54 seconds and the damping ratio in first mode is 2%. For the base-isolated structure, the base stiffness and damping are chosen to achieve the same fundamental natural period of 2.5 seconds and 4% damping ratio in the first mode as in [11]. To calculate the blast loads, the width of the structure is assumed to be 12 meters and the height of each story is assumed to be 3 meters. The model, shown in both fixed-base and base-isolated configurations in Fig. 2.1(a), is a lumped-parameter model with one degree-of-freedom on each story. This model is assumed to remain linear-elastic during all external dynamic excitations. This assumption facilitates a simple study focused on protective systems and is consistent with a scenario where major structural members remain functional while nonstructural components may be damaged.

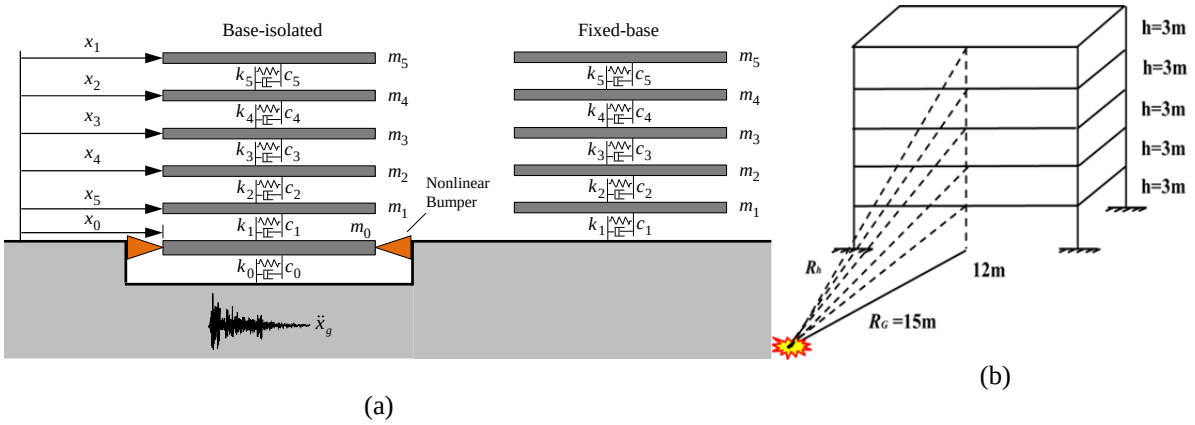

Figure 2.1: (a) Schematic of the 5-story base isolated structure model;
(b) Geometry of the 5-story structure under surface blast load

2.2 Nonlinear Bumpers

The nonlinear bumpers proposed in this study are passive energy dissipation devices consisting of a nonlinear spring with cubic stiffness. By using a cubic stiffness, the device is less effective for smaller excitations, allowing the base isolation device to perform normally. Under larger excitations where damage may occur to the base isolator or a surrounding moat wall, the nonlinear bumpers provide more significant restoring forces. The devices are assumed to provide a restoring force only when they are in compression and fully rebound after the compression. The devices can be either fixed to the base and react against the moat wall or vice versa. One example to realize behavior is to adopt a quarter pyramidal bumper made of the material with high Poisson's ratio [12]. As the bumper is loaded from the tip, the engaging area resisting the compression increases sharply and the bumper exhibits a rapidly increasing stiffness which can produce the desired nonlinearity. In [12], Luo et al. demonstrated that a cubic force-displacement relationship provides a good approximation of an actual quarter pyramidal bumper specimen made from an elastomeric material. The damping effects of the nonlinear bumpers are neglected in this study to both focus on the effect of the added cubic stiffness and not bias the results toward a system with higher damping.

3. EXTERNAL LOADINGS

This section presents the external dynamic excitations applied to the structure systems, including both ground motions and blasts.

3.1 Earthquake Ground Motions

In this study, two strong ground motion records with different magnitudes and frequency content are selected as the input excitations: (1) Northridge (M_w 6.7, 1994): the fault-parallel component recorded at Rinaldi substation and (2) Tohoku Earthquake (M_w 9.0, 2011): the E-W component recorded at MYG004 substation. The first record provides a well-studied earthquake while the latter occurred during the recent 2011 Tohoku Earthquake, which is a high-amplitude, low-frequency, and long duration excitation which can be more demanding for base-isolated structures and other long-period structures.

3.2 Blast Loading

To investigate the performance of base-isolated structures under blast loading, well-established theoretical and empirical equations are used to develop time-history records for the blast forces based on charge weights and standoff distances. Trinitrotoluene (TNT) is selected as the explosive material because blast equations are commonly expressed in equivalent weights of TNT. Explosives with charge weights of 500 kg and 1000 kg of TNT are selected for this study, representing the order of an automobile and van delivery method, respectively [3]. A schematic of the 5-story structure under a surface blast load is shown in Fig. 2.1(b). The points of interest are set at midpoint of each floor due to the lumped-mass assumption made in the model. The detonation is set 15 meters away from the center of the base of the structure. The smallest scaled standoff distance based on this placement and the two charge weights is 1.5 m/kg$^{1/3}$ (3.8 ft/lb$^{1/3}$). Williamson et al. use a maximum of 1.19

m/kg$^{1/3}$ (3 ft/lb$^{1/3}$) to characterize small standoff distances for a series of tests [13], placing scenarios of this paper roughly into a medium to long standoff distance range.

Theoretical and empirical equation-based approaches provide an approximate method to determine the blast pressures or loads on a structure. There are many well-established theoretical and empirical equations to predicting blast characteristics, including estimates for the peak incident and reflected overpressure and other wave parameters [14-18]. Most approaches are based on a cube root scaling law between distance and weight, known as Hopkinson's law [19]. This law states that two different weights of the same explosive W have same blast characteristics Z_h at some scaled distance R_h in similar atmospheric conditions (referencing Eq. 3.2). A theoretical and empirical based approach to developing blast load time histories is selected for this study because: (1) a simplified approach is consistent and compatible with the simplified numerical model selected for the structure and (2) the results are repeatable and easily reproducible.

The procedure for determining the blast wave parameters for the surface blast is shown as follows, referencing the equations of Table 3.1. For all equations, units of m, kg, kPa, and seconds are used for length, mass, pressure, and time respectively.

Step 1: Determine the weight of charge, W , in its TNT equivalent.

Step 2: For the point of interest (e.g., lumped mass location), calculate the standoff distance R_h for height h and distance from the structure R_G , according to Eq. 3.1 and referring to Fig. 2.1(b).

Step 3: Calculate the scaled standoff distance Z_h according to Eq. 3.2.

Step 4: Calculate the peak incident overpressure P_{so} using Eq. 3.3 [17], the peak reflected overpressure P_r using Eq. 3.7 with coefficient C_r given by Eq. 3.8 [16], the arrival time t_A for each point of interest using Eq. 3.6, the positive time duration t_0 using Eq. 3.4 [16], and the wave velocity U using Eq. 3.5 [20]. P_0 is the ambient air pressure (101 kPa typically), and a_0 is the speed of sound in the air taken as 335 m/s.

Step 5: Develop the time history of the pressure wave for each point of interest. The time history can be described as an exponential function in the form of Friedlander's equation [21] as shown in Eq. 3.9, where $P(t)$ is the pressure in time and γ is the parameter controlling the rate of wave amplitude decay which is defined as Eq. 3.10.

Step 6: Calculate the force time histories at each point of interest by multiplying the effective area of each point of interest by the pressure time history at that point.

The resulting story forces due to the 500 kg TNT and 1000 kg TNT blasts are shown in Fig. 3.1. F_{Bb} and F_{B5} are the blast forces applied on the base level and the top floor, respectively.

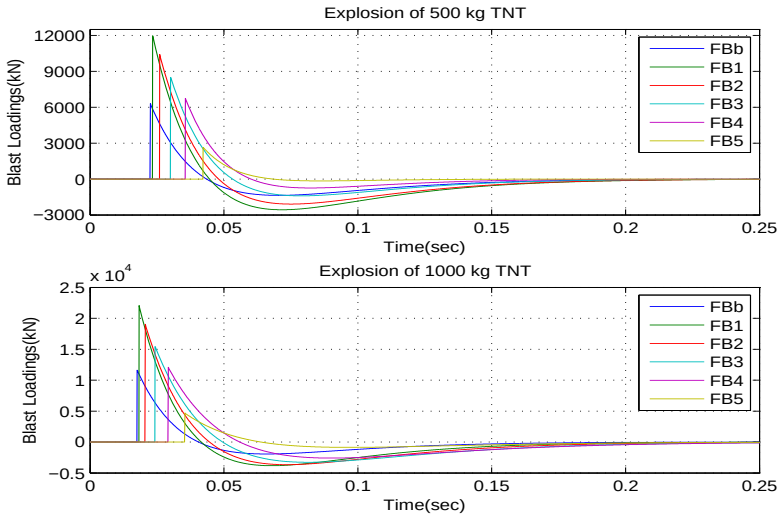

Figure 3.1 Blast loads of 500 kg TNT and 1000 kg TNT on the 5-story structure

Table 3.1 Blast load equations

$R_h = (R_G^2 + h^2)^{1/2}$	(3.1)	$Z_h = R_h / W^{1/3}$	(3.2)
$P_{so} = \frac{1772}{Z_h{}^3} - \frac{114}{Z_h{}^2} + \frac{108}{Z_h}$	(3.3)	$t_o = W^{1/3} 10^{[-2.75+0.27\log(Z_h)]}$	(3.4)
$U = a_0 \cdot \sqrt{(6P_{so} + 7P_0)/7P_0}$	(3.5)	$t_A = R_h / U$	(3.6)
$P_r = C_r \cdot P_{so}$	(3.7)	$C_r = 3\left(\sqrt[4]{P_s/101}\right)$	(3.8)
$P(t) = P_o + P_r(1 - \frac{t}{t_0})\exp(-\gamma \frac{t}{t_0})$	(3.9)	$\gamma = Z_h{}^2 - 3.7Z_h + 4.2$	(3.10)

4. RESULTS AND DATA ANALYSIS

4.1 Evaluation Criteria

To evaluate the performance of different control strategies under blast and seismic loads, the following evaluation criteria are defined based on the maximum and root mean square (RMS) responses of the structure systems.

1. Maximum base displacement shown as Eq. 4.1, where $d_0(t)$ is the base displacement of structure over the time history of each dynamic excitation and t_1 is the duration of the significant response.
2. Maximum RMS base displacement shown as Eq. 4.2.
3. Maximum interstory drift of the superstructure shown as Eq. 4.3, where $d_i(t)$ is the interstory drift of the *i*-th story of the structure over the time history of each dynamic excitation.
4. Maximum RMS interstory drift of the superstructure shown as Eq. 4.4.
5. Maximum story absolute acceleration of the superstructure shown as Eq. 4.5, where $a_i(t)$ is the absolute acceleration of the *i*-th story of the structure over the time history of each dynamic excitation.
6. Maximum RMS story absolute acceleration of the superstructure shown as Eq. 4.6.
7. Maximum base absolute acceleration shown as Eq. 4.7, where $a_0(t)$ is the base absolute acceleration of the structure over the time history of each dynamic excitation.
8. Maximum RMS base absolute acceleration shown as Eq. 4.8.

Table 4.1 Evaluation criteria

$J_1 = \max_{t\in[0,t_1]} \left\| d_0(t) \right\|$	(4.1)	$J_2 = \max_{t\in[0,t_1]} \left\| RMS\left(d_0(t)\right) \right\|$	(4.2)
$J_3 = \max \left\{ \max_{t\in[0,t_1]}^{i=1\to n} \left\| d_i(t) \right\| \right\}$	(4.3)	$J_4 = \max \left\{ \max_{t\in[0,t_1]}^{i=1\to n} \left\| RMS\left(d_i(t)\right) \right\| \right\}$	(4.4)
$J_5 = \max \left\{ \max_{t\in[0,t_1]}^{i=1\to n} \left\| a_i(t) \right\| \right\}$	(4.5)	$J_6 = \max \left\{ \max_{t\in[0,t_1]}^{i=1\to n} \left\| RMS\left(a_i(t)\right) \right\| \right\}$	(4.6)
$J_7 = \max_{t\in[0,t_1]} \left\| a_0(t) \right\|$	(4.7)	$J_8 = \max_{t\in[0,t_1]} \left\| RMS\left(a_0(t)\right) \right\|$	(4.8)

The symbols representing the control systems and the reference systems are listed in Table 4.2. For each control alternative, these criteria are evaluated for all blast and earthquake loads.

Table 4.2 Symbols of different systems

Symbols	Systems
FB	Fixed base structure system
BI	Base isolated structure system containing linear elastomeric bearings only
BI-NLB	Base isolated system with a nonlinear bumper connected to the base

4.2 Performance of Base Isolation under Blast and Seismic Loading

The performances of the fixed-base structure and base-isolated structure are first studied across all blast and earthquake loads. Based on the numerical time history analyses, base isolation improves most evaluation criteria when compared to the fixed-base structure as shown in Fig. 4.1. These results are expected for earthquake ground motions, but the blast loadings warrant closer investigation. Under blast loadings, base isolation performs well in reducing the interstory drift by altering the mode shapes to concentrate deflections at the base. However, there is no reduction to the maximum absolute acceleration of the superstructure. The maximum acceleration comes immediately due to the intense loading and without regard for the structural dynamics (i.e., before the structure can react), thus cannot be reduced though the proposed methods. When instead looking at the RMS absolute acceleration, there is a clear reduction as this metric includes accelerations beyond the initial impulse. Most importantly, base isolation shows promise for global response reduction under blast loading.

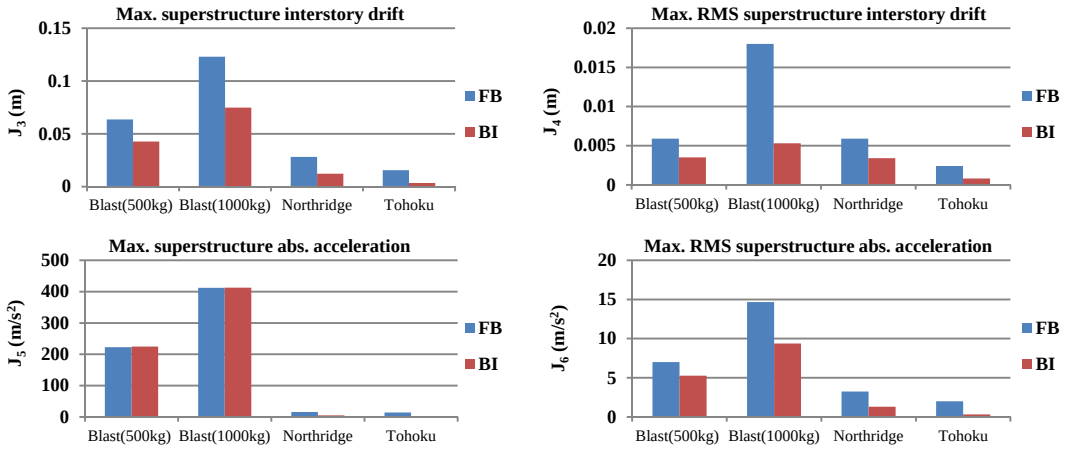

Figure 4.1 Performance of base-isolation under blasts and earthquakes

4.3 Performance Improvements Through Nonlinear Bumpers

This section will explore the performance of base-isolated structures with nonlinear bumpers under blast and earthquake loads alongside fixed-base and base-isolated reference structures. By comparing results to the fixed-base structure, the overall performance of the base-isolated structure plus nonlinear bumpers can be assessed. By comparing results to the base-isolated structure, the improvements made through nonlinear bumpers can be assessed.

Fig. 4.2 presents the normalized maximum values of the controlled systems with supplemental devices under both blasts and earthquakes. Note that the base displacements are normalized to the passive base-isolation systems to highlight the improvements of the supplemental passive devices. The superstructure interstory drifts and absolute accelerations are normalized to the fixed-base systems to demonstrate that the supplemental devices still allow the base-isolated system to function as intended. As can be seen in Fig. 4.2, the base displacements are successfully reduced through the nonlinear bumpers for all excitations. For other criteria, such as superstructure interstory drift and the absolute acceleration, nonlinear bumpers maintain the improvements of the base-isolated system relative to the fixed-base system. The nonlinear bumpers performs best in the reduction of the base displacement under all excitations, but concurrently leads to amplifications on the interstory drift and the absolute acceleration of the structure. This tradeoff is especially pronounced for the Northridge record where significant base displacement reduction is seen at the cost of increased superstructure acceleration. However, even with an amplification compared to the base isolated system, the interstory drift and structural accelerations are still below the responses of the fixed base system. Fig. 4.3 presents the time history of the base displacement, clearly showing that the nonlinear bumpers keep the base displacement under 30 cm for all excitations.

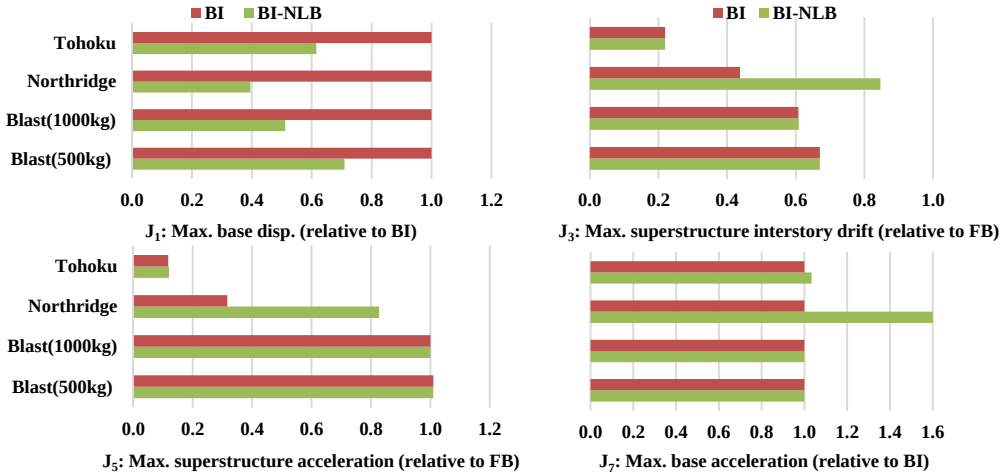

Figure 4.2 Evaluation criteria comparison for different control systems under earthquakes and blasts

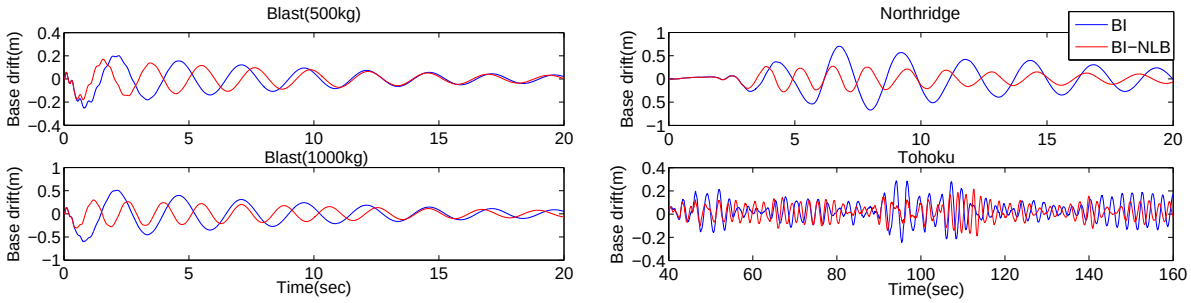

Figure 4.3 Time history of base displacement under multiple excitations

The nonlinear bumpers are designed to allow the base-isolation to perform as intended under low amplitude excitations while restricting damaging base displacements under larger amplitude excitations. Fig. 4.4 shows the performance under different amplitude scaling of the Northridge earthquake to focus on the influence of input amplitude. Under the lower amplitudes, results from the base-isolated structure and the base-isolated structure with nonlinear bumper are quite similar, both offering improvements to the fixed-base structure. Under larger excitations, the nonlinear bumper prevents large base displacements. It is also observed that the interstory drifts and accelerations are maintained at low levels (relative to the fixed base).

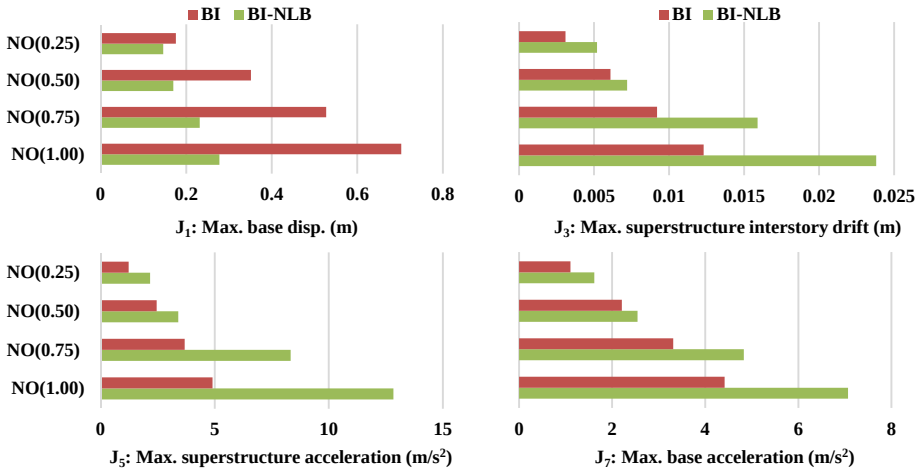

Figure 4.4 Evaluation criteria comparison for different control systems under different levels of Northridge

5. CONCLUSIONS

This study investigated the mitigation of damage under medium to long standoff distance blasts on civil infrastructure through base isolation. The beneficial effects of using base isolation to reduce interstory drifts and absolute story accelerations seen in earthquake engineering were also observed for blast loading. Benefits can be attributed to base isolation producing a more uniform response across all stories, even for a non-uniformly distributed blast loading, by concentrating displacements at the base. Shortcomings of base-isolated structures, namely large base displacement, were considered in the context of both seismic and blast loads. The proposed supplemental control devices were able to maintain nominal base isolation performance under smaller excitations while restrict large base displacements under larger excitations. In general, the supplemental nonlinear bumpers exhibited a favorable reduction in base displacement.

In line with the goals of this study, the potential for base-isolated systems under blast loads were demonstrated and furthermore, supplemental passive devices were able to improve the performance under blast loads while maintaining good performance under seismic excitations. Conclusions are based on numerical simulations of a 5-story structure in fixed-base, base-isolated, and base-isolated with supplemental passive device configurations.

REFERENCES

1. Kinney, G., and Graham, K. (1985). "Explosive shocks in air.", Springer-Verlag.
2. Beshara, F. (1994). "Modelling of blast loading on aboveground structures—I. General phenomenology and external blast." *Computers & Structures*, 51(5), 585-596.
3. NRC (2003). "ISC security design criteria." *National Academies Press, Washington, DC*.
4. Guruprasad, S., and Mukherjee, A. (2000). "Layered sacrificial claddings under blast loading Part II—experimental studies." *International Journal of Impact Engineering*, 24(9), 975-984.
5. Hanssen, A., Enstock, L., and Langseth, M. (2002). "Close-range blast loading of aluminium foam panels." *International Journal of Impact Engineering*, 27(6), 593-618.
6. Kelly, J. "State-of-the-art and state-of-the-practice in base isolation." *Proc., Seminar on Seismic Isolation, Passive Energy Dissipation and Active Control (ATC-17-1), Applied Technology Council, Redwood City*.
7. Kelly, J., Leitmann, G., and Soldatos, A. (1987). "Robust control of base-isolated structures under earthquake excitation." *Journal of Optimization Theory and Applications*, 53(2), 159-180.
8. Kelly, J. M. (1993). *Earthquake-resistant design with rubber*, Springer.
9. Kelly, J. M. (1999). "The role of damping in seismic isolation." *Earthquake engineering & structural dynamics*, 28(1), 3-20.
10. Nagarajaiah, S., and Ferrell, K. (1999). "Stability of elastomeric seismic isolation bearings." *Journal of Structural Engineering*, 125(9), 946-954.
11. Johnson, E. A., Ramallo, J. C., Spencer Jr., B. F., and Sain, M. K. "Intelligent base isolation systems." *Proc., Proceedings of the Second World Conference on Structural Control*, 367-376.
12. Luo, J., Wierschem, N. E., Fahnestock, L. A., Spencer, B. F., Quinn, D. D., McFarland, D. M., Vakakis, A. F., and Bergman, L. A. (2014). "Design, simulation, and large‐scale testing of an innovative vibration mitigation device employing essentially nonlinear elastomeric springs." *Earthquake Engineering & Structural Dynamics*, 43(12), 1829-1851.
13. Williamson, E. B. (2010). *Blast-resistant highway bridges: Design and detailing guidelines*, Transportation Research Board.
14. DoD. (2008). "Explosives Safety Standards." *DoD Manual*, 6055.
15. Brode, H. L. (1955). "Numerical solutions of spherical blast waves." *Journal of Applied physics*, 26(6), 766-775.
16. Lam, N., Mendis, P., and Ngo, T. (2004). "Response spectrum solutions for blast loading." *Electronic Journal of Structural Engineering*, 4, 28-44.
17. Mills, C. "The design of concrete structure to resist explosions and weapon effects." *Proc., Proceedings of the 1st Int. Conference on concrete for hazard protections*, 61-73.
18. Newmark, N., and Hansen, R. (1961). "Design of blast resistant structures." *Shock and Vibration Handbook*, 3.
19. Baker, W. E. (1973). *Explosions in air*, University of Texas Press.
20. Rankine, W. M. (1870). "On the thermodynamic theory of waves of finite longitudinal disturbance." *Philosophical Transactions of the Royal Society of London*, 277-288.
21. Bulson, P. S. (2002). *Explosive loading of engineering structures*, CRC Press.